

## Strengthening of ocean heat uptake efficiency associated with the recent climate hiatus

Masahiro Watanabe,<sup>1</sup> Youichi Kamae,<sup>2</sup> Masakazu Yoshimori,<sup>1</sup> Akira Oka,<sup>1</sup> Makiko Sato,<sup>3,4</sup> Masayoshi Ishii,<sup>5</sup> Takashi Mochizuki,<sup>6</sup> and Masahide Kimoto<sup>1</sup>

Received 30 March 2013; revised 5 May 2013; accepted 6 May 2013; published 17 June 2013.

[1] The rate of increase of global-mean surface air temperature (SAT<sub>g</sub>) has apparently slowed during the last decade. We investigated the extent to which state-of-the-art general circulation models (GCMs) can capture this hiatus period by using multimodel ensembles of historical climate simulations. While the SAT<sub>g</sub> linear trend for the last decade is not captured by their ensemble means regardless of differences in model generation and external forcing, it is barely represented by an 11-member ensemble of a GCM, suggesting an internal origin of the hiatus associated with active heat uptake by the oceans. Besides, we found opposite changes in ocean heat uptake efficiency ( $\kappa$ ), weakening in models and strengthening in nature, which explain why the models tend to overestimate the SAT<sub>g</sub> trend. The weakening of  $\kappa$  commonly found in GCMs seems to be an inevitable response of the climate system to global warming, suggesting the recovery from hiatus in coming decades. **Citation:** Watanabe, M., Y. Kamae, M. Yoshimori, A. Oka, M. Sato, M. Ishii, T. Mochizuki, and M. Kimoto (2013), Strengthening of ocean heat uptake efficiency associated with the recent climate hiatus, *Geophys. Res. Lett.*, 40, 3175–3179, doi:10.1002/grl.50541.

### 1. Introduction

[2] Global-mean surface air temperature (SAT<sub>g</sub>), a simple measure for monitoring long-term change in climate, has been increasing continuously over the last century, albeit with decadal-scale fluctuations. This increase, at least from the 1980s onward, can “very likely” be attributed to human-induced changes in greenhouse gasses (GHGs) [Intergovernmental Panel on Climate Change (IPCC), 2007]. Therefore, it is puzzling that SAT<sub>g</sub> increased little during the first decade of the 21<sup>st</sup> century [Easterling and Wehner, 2009, hereafter EW09], a period often referred to as

a climate hiatus, the cause of which is still under debate. Possible reasons for this hiatus can be classified according to whether they are caused by external or internal forces: increased stratospheric sulfur aerosols [Solomon *et al.*, 2011] and a prolonged minimum phase of the 11-year solar cycle [Kaufmann *et al.*, 2011] are typical explanations for the externally driven hiatus, while the decline of stratospheric water vapor [Solomon *et al.*, 2010] and active ocean heat uptake associated with the negative phase of the Pacific decadal oscillation [Mochizuki *et al.*, 2010; Meehl *et al.*, 2011; Meehl and Teng, 2012] may be attributable to natural fluctuations.

[3] The implications of this hiatus for the retardation of global warming have been examined extensively. Global energy budgets indicate a continuous excess of the top of atmosphere (TOA) radiative energy input for the last two decades [Trenberth and Fasullo, 2010; Hansen *et al.*, 2011]; it suggests that Earth’s surface should have warmed unless energy was further carried into subsurface oceans. In fact, recent ocean temperature data sets have consistently exhibited a robust warming of the global upper ocean in the early 21<sup>st</sup> century [Levitus *et al.*, 2012; Lyman *et al.*, 2012; Gleckler *et al.*, 2012]. Balmaseda *et al.* [2013] emphasized the heat absorbed in the deeper ocean layers below 700 m, significantly contributing to the global energy budgets in the last decade. Therefore, the flattening of SAT<sub>g</sub> anomalies after 2000 does not necessarily reflect a slowing of global warming.

[4] To date, the warming trend of SAT<sub>g</sub> throughout the 20<sup>th</sup> century has been reproduced well by an ensemble of general circulation models (GCMs) to which known external forcing agents have been applied [IPCC, 2007]. However, an attribution study by Stott and Jones [2012] suggests that GCMs tend to overestimate the warming after around 2000. Because questions regarding the uncertainty and reliability of simulations of past and future climate by GCMs have been raised from outside the modeling community, a rigorous test of the extent to which GCMs can capture the recent hiatus period is critical in proving the fidelity of climate change simulations. For this purpose, here we analyze observed data and results of multimodel ensembles (MMEs) obtained from the Coupled Model Intercomparison Project Phase 5 (CMIP5) [Taylor *et al.*, 2012] and an older phase (CMIP3) [Meehl *et al.*, 2007]. This work may partly be an extension of EW09, but we examine not only SAT<sub>g</sub> linear trends but also subsurface ocean heat content and global energy budgets to investigate consistency between the hiatus period and ocean heat uptake.

### 2. Model and Analysis Method

[5] We use surface air temperature (SAT) data compiled at the Hadley Centre and the Climate Research Unit, University of East Anglia, referred to as HadCRUT4 [Kennedy *et al.*,

Additional supporting information may be found in the online version of this article.

<sup>1</sup>Atmosphere and Ocean Research Institute, the University of Tokyo, Kashiwa, Chiba, Japan.

<sup>2</sup>National Institute for Environmental Studies, Tsukuba, Ibaraki, Japan.

<sup>3</sup>NASA Goddard Institute for Space Studies, New York, NY, USA.

<sup>4</sup>Columbia University Earth Institute, New York, New York, USA.

<sup>5</sup>Meteorological Research Institute, Japan Meteorological Agency, Tsukuba, Ibaraki, Japan.

<sup>6</sup>Japan Agency for Marine-Earth Science and Technology, Yokohama, Kanagawa, Japan.

Corresponding author: M. Watanabe, Atmosphere and Ocean Research Institute, University of Tokyo, Kashiwa, Chiba 277-8568, Japan. (hiro@aori.u-tokyo.ac.jp)

©2013. American Geophysical Union. All Rights Reserved. 0094-8276/13/10.1002/grl.50541

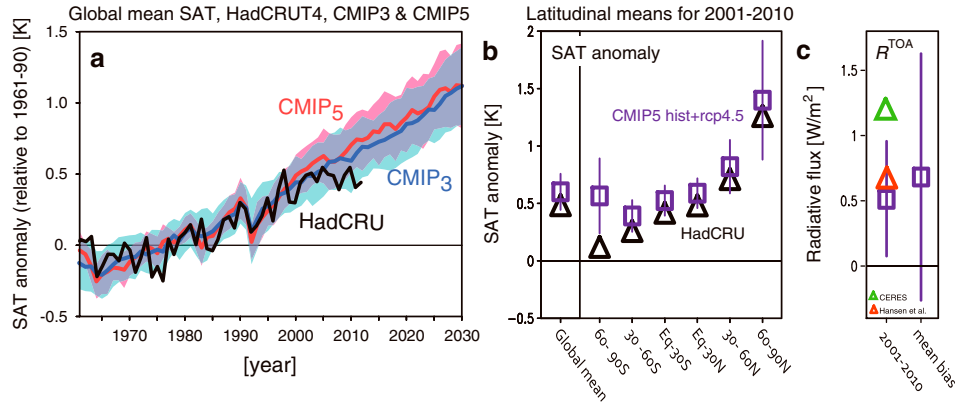


**Figure 1.**  $SAT_g$  anomalies relative to 1961–1990 means in observations and CMIP models. (a) Observed record (black curve) taken from HadCRUT4 and the simulations based on the ensemble averages of 20<sup>th</sup> century historical experiments of CMIP3 (blue) and CMIP5 (red) models. The standard deviation ( $\sigma$ ) of the ensemble average is denoted by shading. The model values after 2000 and 2006 for CMIP3 and CMIP5 are from the A1b and RCP4.5 emission scenario runs, respectively. (b) 10 year mean  $SAT_g$  anomalies for 2001–2010 averaged globally and over the six latitudinal bands. CMIP5 model ensemble means are indicated by squares, with the spread represented by vertical lines. (c) The global-mean  $R^{TOA}$  for 2001–2010. The estimates from CERES EBAF data and by Hansen *et al.* [2011] are shown by green and red triangles, respectively. The energy budget is not closed in GCMs, so that the mean bias in  $R^{TOA}$  defined by the long-term average in the piControl experiments (right) has been extracted in advance.

2011] and obtained from 24 and 22 MMEs of CMIP3 and CMIP5, respectively (see Table S1 in the auxiliary material for individual models). The 20<sup>th</sup> century historical experiments are concatenated with A1b and RCP4.5 scenario experiments after 2006 and 2001 for CMIP3 and CMIP5. Although different scenarios adopt different future GHG emission pathways, the near-future climate depends little on the choice of emission scenario [Hawkins and Sutton, 2009].

[6] In addition to the above single-member MMEs, we analyze ensembles adopting different initial conditions for several CMIP5 models: CanCM4, CNRM-CM5, CSIRO Mk-3.6, HadCM3, and MIROC5. Three models (CanCM4, CSIRO Mk-3.6, and HadCM3) have 10 members for historical and RCP4.5 experiments. CNRM-CM5 also has 10 members for the historical run but provides a single member for RCP4.5, so that the ensemble spread after 2005 is not defined. For MIROC5, five members for the historical and RCP4.5 runs were available in the CMIP5 archive, but we made additional six members branched off in January 1950 and integrated up to 2020.

[7] All analyses are based on the annual-mean anomaly fields defined as deviation from the climatology for 1961–1990. The CMIP outputs and HadCRUT4 data are first regridded to a  $2.5 \times 2.5^\circ$  resolution; then,  $SAT_g$  is calculated using the HadCRUT4 grid mask. We also used the Goddard Institute for Space Studies Surface Temperature Analysis data [Hansen *et al.*, 2010] to evaluate observational uncertainty, but presented only the results with HadCRUT4.

### 3. Results

#### 3.1. $SAT_g$ Trends in Observations and GCMs

[8] Figure 1a compares the annual-mean  $SAT_g$  time series from the CMIP MMEs and observations of HadCRUT4. Both the CMIP3 and CMIP5 models reproduce well the observed  $SAT_g$  before 2000 but indicate monotonic warming afterward, without hiatus. For the CMIP5 ensemble average, the root-mean-square error of  $SAT_g$  is 0.16 K for 2001–2012, 88% larger than that for 1991–2000. Thus, the GCMs

do not capture the recent hiatus, in the ensemble-mean sense, regardless of differences in model generation and external forcing. The errors in  $SAT_g$  anomaly for 2001–2010 (0.62 K in GCMs versus 0.49 K in observations) come from all latitudinal bands (Figure 1b). It appears that the error is particularly large over southern high latitudes, where little warming occurs in observations. However, the surface measurements are fewest over the Southern Oceans; therefore, uncertainty remains. Even if the observations in this region are reliable, the area-weighted  $SAT_g$  anomalies indicate that the error at  $60^\circ$ – $90^\circ$ S accounts for 18% of the  $SAT_g$  error, which is less than the fraction explained by the tropical error (36% at  $30^\circ$ S– $30^\circ$ N).

[9] The TOA radiative budgets measure if the climate system gains excessive energy. In GCMs, the TOA net energy imbalance ( $R^{TOA}$ , positive downward), after removal of mean bias defined using the preindustrial control (piControl) simulation, shows a net energy gain of  $0.51 \pm 0.44 \text{ W m}^{-2}$  during 2001 and 2010 (Figure 1c). The satellite estimate obtained from the Clouds and Earth’s Radiant Energy System (CERES) data [Loeb *et al.*, 2009] reveals  $R^{TOA} = 1.19 \text{ W m}^{-2}$ , more than double the model ensemble mean. Because CERES data indicate a spuriously large positive  $R^{TOA}$  in 2008–2009, which leads to a shortfall in the Earth’s energy budgets [Trenberth and Fasullo, 2010], we also use the TOA net energy budgets estimated by Hansen *et al.* [2011]. Their data indicated that  $R^{TOA} = 0.66 \text{ W m}^{-2}$ , which is closer to, but still slightly larger than, the model value. This implies that errors in the external forcing agents, even if they exist, do not explain the overestimation of the  $SAT_g$  trend for 2001–2010.

[10] The climate system can give rise to slow natural fluctuations that accompany a transient surface cooling, and these are sometimes seen in long climate simulations by a single GCM [EW09; Meehl *et al.*, 2011]. The possibility that the hiatus after 2000 happened by chance is unlikely to explain the difference between the model and observations in Figure 1a, because none of the models represents the adventitious hiatus of 1996–2010 (Figure S1). However, the 22 CMIP5 models may be far from representing a true probability

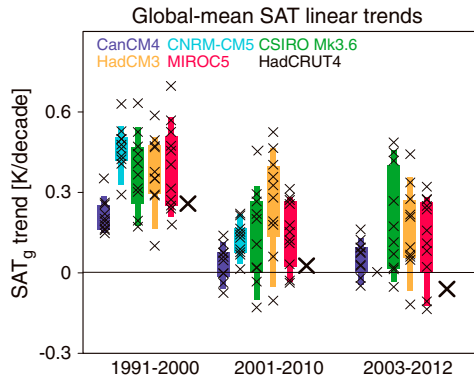


**Figure 2.** SAT<sub>g</sub> trends during the last two decades for 1991–2000 (left), 2001–2010 (middle), and 2003–2012 (right). Thick “cross” marks indicate the observational linear trends, while thin marks represent the trends in historical ensembles from the five CMIP5 models having more than 10 members. Thick (thin) bars denote the 50% (75%) range of the trend values in each ensemble.

distribution for the decadal SAT<sub>g</sub> anomaly. Therefore, we use five models that have more than 10 members of the historical and RCP4.5 simulations to take a closer look at the recent SAT<sub>g</sub> linear trends (Figure 2). Two model ensembles (CNRM-CM5 and CanCM4) exhibit a narrow spread, which means that they may not encompass a sufficient range of natural fluctuations. The remaining three ensembles (CSIRO Mk-3.6, HadCM3, and MIROC5) include the observed SAT<sub>g</sub> linear trend for 1991–2000 (0.26 K per decade) in a 50th percentile, and for 2001–2010 (0.03 K per decade) in a lower 50–75th percentile. The discrepancy appears small, but it becomes larger when we include the latest two years of 2011–2012 in the estimate. The large spread of more than 0.3 K in the three ensembles suggests that the observed hiatus was due to a large natural fluctuation and/or the GCMs are systematically biased to produce a warmer surface for a particular reason.

### 3.2. Natural Internal Fluctuations and Hiatus

[11] To investigate whether the difference between the modeled and observed 2001–2010 SAT<sub>g</sub> trends results from natural internal variability, we focus on the 11-member ensemble by MIROC5 [Watanabe et al., 2010]. The 2001–2010 SAT<sub>g</sub> linear trends in MIROC5 range from –0.04 to 0.28 K per decade, indicating that some members reproduce the hiatus (Figure 2). A comparison of the zonal-mean ocean temperature anomaly between observations by Ishii and Kimoto [2009] and the MIROC5 ensemble average reveals that the model reproduces well the latitude-depth structure of ocean warming (Figure S2). The warming penetrates into the subsurface below 300 m at around 65°N and 50°S, while subsurface cooling is observed in the low-latitude oceans.

[12] A pattern of internal variability responsible for the occurrence of hiatus can be identified by a linear regression of 2001–2010 sea surface temperature (SST) anomalies on the 2001–2010 SAT<sub>g</sub> anomaly after subtraction of the respective ensemble means. Among 11 members, the decadal-means in SAT<sub>g</sub> anomalies are highly correlated with the SST anomaly over the Pacific (Figure 3a), where the pattern resembles a negative phase of the Pacific decadal oscillation [Mochizuki et al., 2010] and is also very similar to the SST anomaly pattern during the hiatus period in another GCM [Meehl et al., 2011, 2013]. To examine whether the internal variability consistently explains the model errors in ocean states, we applied a simple statistical correction using this significant relationship to the ensemble-mean SST and heat content anomalies for 2001–2010 (see also Figure S3 illustrating the rationale of the correction). For the ensemble average  $\langle x \rangle$  and the deviation from the ensemble average  $x'$ , corrected ensemble average  $\langle x \rangle^*$  is written as  $\langle x \rangle^* = \langle x \rangle + \partial x' / \partial SAT'_g (SAT_g^{obs} - \langle SAT_g \rangle)$ , where  $x$  is either SST or heat content anomaly at each grid and  $SAT_g^{obs}$  denotes the observed SAT<sub>g</sub> anomaly. The derivative is given by the regression slope in the 11-member ensemble. Note that, by definition,  $\langle SAT_g \rangle^* = SAT_g^{obs}$ .

[13] The global-mean SST anomaly for 2001–2010 is corrected from 0.38 to 0.28 K, approaching the observed value of 0.26 K. In MIROC5, the ensemble-mean ocean heat

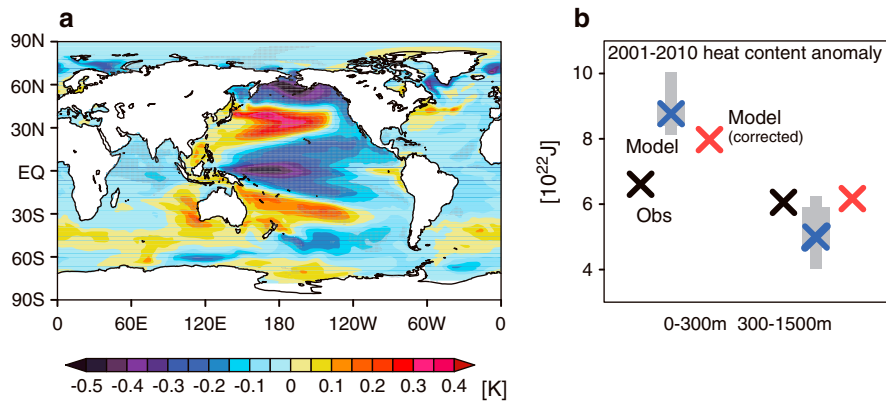


**Figure 3.** Natural ocean heat uptake variability and correction to simulated decadal-mean anomalies for 2001–2010. (a) Linear regression of the decadal-means of SST anomalies on the SAT<sub>g</sub> anomaly among 11-member ensemble historical and RCP4.5 experiments by MIROC5. The ensemble means have been subtracted and the values indicate the SST anomaly per  $-\sigma$  of SAT<sub>g</sub> anomaly. Regressed anomalies significant at the 95% level are stippled. (b) Global-mean HC<sub>300</sub> and HC<sub>1500</sub> anomalies for 2001–2010, including observational data [Ishii and Kimoto, 2009] (black), ensemble mean of the MIROC5 simulation (blue), and the corrected ensemble mean (red). Thick and thin gray bars indicate 50% and 75% ranges of the ensemble, respectively.

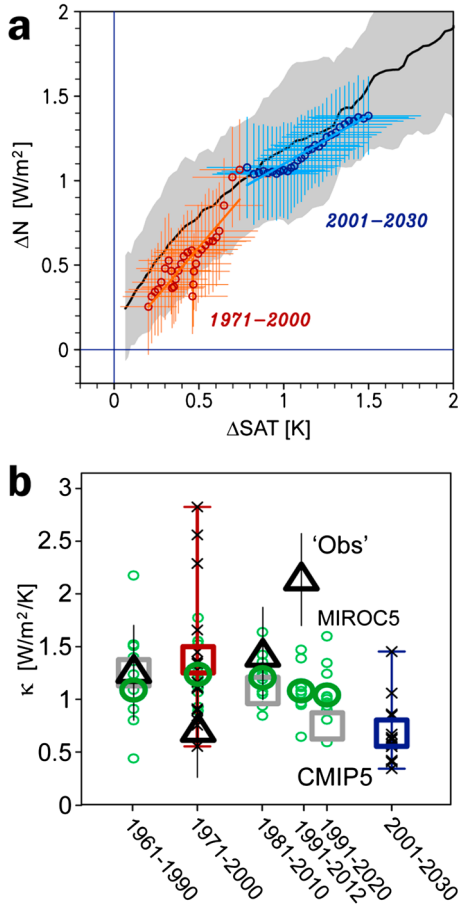


**Figure 4.** Estimates of  $\kappa$  from CMIP5 models and observational data. (a) Scatterplot of  $\Delta N$  against  $\Delta T$  in CMIP5 models for 1971–2000 (red) and 2001–2030 (blue). Both variables are smoothed using an 11 year running mean. The error bars and lines indicate  $\pm 1\sigma$  and least-squares fits, respectively. Black curve with grey shading represents the evolution in the transient experiments with  $\text{CO}_2$  increasing at 1% per year and its 95% confidence limit. (b) Estimate of  $\kappa$  with 30 year window from 1961 to 2030 in CMIP5 models (squares), from 1961 to 2020 in MIROC5 (circles), and from 1961 to 2012 in combination of HadCRUT4  $\text{SAT}_g$ ,  $F$  by Hansen *et al.* [2011], and a range of  $\lambda$  in CMIP5 models substituted to equation (1) (triangles with vertical lines). For 1971–2000 (red) and 2001–2030 (blue) CMIP5 models, the ensemble-mean values are identical to the regression slopes in Figure 4a, and the estimates from individual models are indicated by “cross” marks (the maximum and minimum are denoted by error bars).

content anomalies for the upper 300 m ( $\text{HC}_{300}$ ) anomaly is overestimated whereas the heat content anomalies for deeper layers between 300 and 1500 m ( $\text{HC}_{1500}$ ) is underestimated for 2001–2010, indicating weaker heat uptake below 300 m (Figure 3b, black and blue symbols). When the correction is applied to the global-mean  $\text{HC}_{300}$  and  $\text{HC}_{1500}$ , it results in an enhanced heat uptake as represented by the smaller  $\text{HC}_{300}$  (larger  $\text{HC}_{1500}$ ) anomaly, supporting the internal origin of the hiatus (Figure 3b, red). The nature of the internal variability associated with the hiatus period is also examined using the piControl run. In short, the SST anomaly pattern shown in Figure 3a has some similarities to the internally generated hiatus in MIROC5, in which tropical cooling is

caused by a strengthening of equatorial upwelling above 500 m. However, the decadal  $\text{HC}_{300}$  variability in observations and historical runs is, unlike in piControl run, controlled partly by external forcing such as volcanic eruptions (see text and Figures S4–S5 in the auxiliary material).

### 3.3. Slow Change in the Ocean Heat Uptake Efficiency

[14] Changes in ocean heat uptake could generate the hiatus period regardless of its origin. Conversely, it has been shown repeatedly that GCMs tend to overestimate the observed ocean heat uptake [IPCC, 2007; Knutti and Tomassini, 2008; Boé *et al.*, 2009]. Therefore, it is paradoxical that models systematically overestimate the  $\text{SAT}_g$  trend for 2001–2010. Ocean heat uptake consists of vertical advection, diffusion, and convective mixing, which work differently at different latitudes [Gregory, 2000], and therefore, investigation of individual oceanic processes in observational data is difficult. Instead, we examine the above paradox by means of an approximated form of a two-box energy balance model for surface and deep ocean temperatures [Held *et al.*, 2010; Geoffroy *et al.*, 2012] (see auxiliary material for the derivation).

$$\Delta N = \Delta F - \lambda \Delta T \approx \kappa \Delta T, \quad (1)$$

where  $N$  denotes the surface net energy imbalance over oceans,  $\lambda$  is the climate feedback parameter, and  $\kappa$  indicates the heat uptake efficiency coefficient [Gregory and Mitchell, 1997]. The TOA radiative forcing,  $F$ , is time-dependent, and  $\Delta$  indicates changes from the preindustrial climate, defined as the 1851–1900 average. The expression of heat uptake in equation (1) is *a posteriori*, and will be acceptable only for transient forced response. Moreover,  $\kappa$  has been assumed to be constant for simplicity but varies empirically in time [Raper *et al.*, 2002]. In the literature, another parameter known as the efficacy factor,  $\epsilon$ , is sometimes introduced to the energy balance model to represent the dependence of climate feedback on the geographical distribution of temperature increase associated with ocean heat uptake [Held *et al.*, 2010; Winton *et al.*, 2010]. The nonconstant  $\kappa$  is equivalent to introducing  $\epsilon$ , but is used here because we do not assume the specific pattern in  $\Delta T$  necessary for arguing the efficacy change.

[15] When equation (1) is applied to 16 CMIP5 models,  $\Delta N$  is shown to be linearly related with  $\Delta \text{SAT}_g$  but with different regression slopes, namely,  $\kappa$ , for different periods: 1.38 and  $0.68 \text{ W m}^{-2} \text{ K}^{-1}$  for 1971–2000 and 2001–2030, respectively (Figure 4a). Owing to interannual and decadal fluctuations in  $\Delta N$  and  $\Delta \text{SAT}_g$ , we estimate long-term change in  $\kappa$  with a 30 year moving window, the results of which indicate a gradual decrease from 1961 to 2030 in CMIP5 models (squares) and the 11-member MIROC5 ensemble (green circles) in Figure 4b. Although direct measurements of  $\Delta N$  are not available, equation (1) can be applied to observations partly:  $F$  of Hansen *et al.* [2011], HadCRUT4  $\text{SAT}_g$ , and  $\lambda$  derived from CMIP5 models [Andrews *et al.*, 2012]. The range of  $\lambda$  corresponding to equilibrium climate sensitivities of 2.1–4.7 K ( $0.63$ – $1.52 \text{ W m}^{-2} \text{ K}^{-1}$ ) gives the uncertainty of our estimate. The result indicates that  $\kappa$  is similar to the direct estimate from GCMs for 1971–2000, but in the observations (triangles) it is clearly strengthened after this time contrasting to GCMs (squares in Figure 4b). This discrepancy is consistent with the systematic warming bias in the  $\text{SAT}_g$  trends in GCMs (Figures 1, 2). The larger  $\kappa$  in observations indicates greater mixing of heat into the deeper ocean layers and less surface warming in the hiatus.

#### 4. Concluding Discussion

[16] Given that  $\Delta N$  is equal to the heat content tendency, our evaluation of “observational”  $\kappa$  can be verified using heat content data. Qualitatively, the fact that the upper-ocean heat content is shown to increase continuously after 2000 [Levitus et al., 2012; Balmaseda et al., 2013] means that no weakening of  $\kappa$  will have occurred; this is consistent with our estimate. On the other hand, the weakening tendency of  $\kappa$  in GCMs is seen in the concomitant transient experiments in which CO<sub>2</sub> is increased at 1% per year (black curve in Figure 4a) and also in individual models (Figure S6), so that it is an intrinsic characteristic of the climate system forced by GHG increase. Because climate will be far from equilibrium during this period, the weakening in  $\kappa$  should not be interpreted as saturation of heat uptake. Rather, it is likely that surface warming gradually stabilizes ocean stratification, thus reducing deep-water production at high latitudes, which acts to weaken advective heat uptake by meridional overturning circulation [cf. Meehl et al., 2011, 2013].

[17] It is not yet clear why the heat uptake efficiency is strengthened in nature. Although the enhancement of heat uptake could be induced by natural variability (Figure 3), consistent with better reproduction of hiatus with initialized hindcast experiments [Meehl and Teng, 2012; Guemas et al., 2013], it could also be the result of anthropogenic forcing. In the Southern Hemisphere, surface heat appears to penetrate at around 50°S (Figure S2), where the wind-induced Ekman downwelling may have intensified in recent decades in association with stratospheric ozone depletion [Thompson and Solomon, 2002]. We cannot yet conclude whether the observed hiatus was part of unpredictable natural phenomena or a deterministic response to predictable changes in external forcing agents. However, the decrease of  $\kappa$  represents a physically based response of the climate system to GHG increase, as inferred from the results in GCMs. Therefore, unless models miss effects of other forcing agents, it is likely that this process will occur and act to accelerate surface warming in coming decades.

[18] **Acknowledgments.** The authors are grateful to G. A. Meehl and an anonymous reviewer for their encouraging comments. This work was supported by the Program for Risk Information on Climate Change (SOUSEI project) and Grants-in-Aid 23310014 and 23340137 from MEXT, Japan.

[19] The Editor thanks Gerald Meehl and an anonymous reviewer for their assistance in evaluating this paper.

#### References

Andrews, T., J. M. Gregory, M. J. Webb, and K. E. Taylor (2012), Forcing, feedbacks and climate sensitivity in CMIP5 coupled atmosphere–ocean climate models, *Geophys. Res. Lett.*, *39*, L09712, doi:10.1029/2012GL051607.

Balmaseda, M. A., K. E. Trenberth, and K. E. Kallen (2013), Distinctive climate signals in the reanalysis of global ocean heat content, *Geophys. Res. Lett.*, doi:10.1002/grl.50382, in press.

Boć, J., A. Hall, and X. Qu (2009), Deep ocean heat uptake as a major source of spread in transient climate change simulations, *Geophys. Res. Lett.*, *36*, L22701, doi:10.1029/2009GL040845.

Easterling, D. R., and M. F. Wehner (2009), Is the climate warming or cooling? *Geophys. Res. Lett.*, *36*, L08706, doi:10.1029/2009GL037810.

Geoffroy, O., D. Saint-Martin, and A. Ribes (2012), Quantifying the sources of spread in climate change experiments, *Geophys. Res. Lett.*, *39*, L24703, doi:10.1029/2012GL054172.

Gleckler, P. J., et al. (2012), Human-induced global ocean warming on multidecadal timescales, *Nat. Clim. Change*, *2*, 524–529.

Gregory, J. M. (2000), Vertical heat transports in the ocean and their effect on time-dependent climate change, *Clim. Dyn.*, *16*, 501–515.

Gregory, J. M., and J. F. B. Mitchell (1997), The climate response to CO<sub>2</sub> of the Hadley Centre coupled AOGCM with and without flux adjustment, *Geophys. Res. Lett.*, *24*, 1943–1946.

Guemas, V., F. J. Doblas-Reyes, I. Andreu-Burillo, and M. Asif (2013), Retrospective prediction of the global warming slowdown in the past decade, *Nat. Clim. Change*, doi:10.1038/nclimate1863.

Hansen, J., R. Ruedy, M. Sato, and K. Lo (2010), Global surface temperature change, *Rev. Geophys.*, *48*, RG4004, doi:10.1029/2010RG000345.

Hansen, J., M. Sato, P. Kharecha, and K. von Schuckmann (2011), Earth’s energy imbalance and implications, *Atmos. Chem. Phys.*, *11*, 13421–13449.

Hawkins, E., and R. Sutton (2009), The potential to narrow uncertainty in regional climate predictions, *Bull. Am. Meteorol. Soc.*, *90*, 1095–1107.

Held, I. M., et al. (2010), Probing the fast and slow components of global warming by returning abruptly to preindustrial forcing, *J. Clim.*, *23*, 2418–2427.

Intergovernmental Panel on Climate Change (2007), *The Fourth Assessment Report of the Intergovernmental Panel on Climate Change*, edited by S. Solomon, et al., Cambridge Univ Press, Cambridge, UK.

Ishii, M., and M. Kimoto (2009), Reevaluation of historical ocean heat content variations with time-varying XBT and MBT depth bias corrections, *J. Oceanogr.*, *65*, 287–299.

Kaufmann, R. K., H. Kauppi, M. L. Mann, and J. H. Stock (2011), Reconciling anthropogenic climate change with observed temperature 1998–2008, *Proc. Natl. Acad. Sci.*, *108*, 11790–11793.

Kennedy, J. J., N. A. Rayner, R. O. Smith, M. Saunby, and D. E. Parker (2011), Reassessing biases and other uncertainties in sea-surface temperature observations measured in situ since 1850. Part 2: biases and homogenization, *J. Geophys. Res.*, *116*, D14104, doi:10.1029/2010JD015220.

Knutti, R., and L. Tomassini (2008), Constraints on the transient climate response from observed global temperature and ocean heat uptake, *Geophys. Res. Lett.*, *35*, L09701, doi:10.1029/2007GL032904.

Levitus, S., et al. (2012), World ocean heat content and thermocline sea level change (0–2000 m), 1955–2010, *Geophys. Res. Lett.*, *39*, L10603, doi:10.1029/2012GL051106.

Loeb, N. G., et al. (2009), Toward optimal closure of the earth’s top-of-atmosphere radiation budget, *J. Clim.*, *22*, 748–766.

Lyman, J. M., et al. (2012), Robust warming of the global upper ocean, *Nature*, *465*, 334–337.

Meehl, G. A., and H. Teng (2012), Case studies for initialized decadal hindcasts and predictions for the Pacific region, *Geophys. Res. Lett.*, *39*, L22705, doi:10.1029/2012GL053423.

Meehl, G. A., et al. (2007), The WCRP CMIP3 multimodel dataset: A new era in climate change research, *Bull. Am. Meteorol. Soc.*, *88*, 1383–1394.

Meehl, G. A., J. M. Arblaster, J. T. Fasullo, A. Hu, and K. E. Trenberth (2011), Model-based evidence of deep-ocean heat uptake during surface-temperature hiatus periods, *Nat. Clim. Change*, *1*, 360–364.

Meehl, G. A., A. Hu, J. M. Arblaster, J. Fasullo, and K. E. Trenberth (2013), Externally forced and internally generated decadal climate variability associated with the Interdecadal Pacific Oscillation, *J. Clim.*, <http://dx.doi.org/10.1175/JCLI-D-12-00548.1>, in press.

Mochizuki, T., et al. (2010), Pacific decadal oscillation hindcasts relevant to near-term climate prediction, *Proc. Natl. Acad. Sci.*, *107*, 1833–1837.

Raper, S. C. B., J. M. Gregory, and R. J. Stouffer (2002), The role of climate sensitivity and ocean heat uptake on AOGCM transient temperature response, *J. Clim.*, *15*, 124–130.

Solomon, S., et al. (2010), Contributions of stratospheric water vapor to decadal changes in the rate of global warming, *Science*, *327*, 1219–1223.

Solomon, S., et al. (2011), The persistently variable “background” stratospheric aerosol layer and global climate change, *Science*, *333*, 866–870.

Stott, P. A., and G. S. Jones (2012), Observed 21st century temperatures further constrain likely rates of future warming, *Atmos. Sci. Lett.*, *13*, 151–156.

Taylor, K. E., et al. (2012), An overview of CMIP5 and the experiment design, *Bull. Am. Meteorol. Soc.*, *93*, 485–498.

Thompson, D. W. J., and S. Solomon (2002), Interpretation of recent Southern Hemisphere climate change, *Science*, *296*, 895–899.

Trenberth, K. E., and J. T. Fasullo (2010), Tracking Earth’s energy, *Science*, *328*, 316–317.

Watanabe, M., et al. (2010), Improved climate simulation by MIROC5: Mean states, variability, and climate sensitivity, *J. Clim.*, *23*, 6312–6335.

Winton, M., K. Takahashi, and I. M. Held (2010), Importance of ocean heat uptake efficacy to transient climate change, *J. Clim.*, *23*, 2333–2344.